THE EUROPEAN
PHYSICAL JOURNAL C

CrossMark

Pion couplings to the scalar B meson

Benoît Blossier[1,a], **Nicolas Garron**[2,b], **Antoine Gérardin**[1,3]

[1] Laboratoire de Physique Théorique, Unité Mixte de Recherche 8627 du Centre National de la Recherche Scientifique, CNRS et Université Paris-Sud XI, Bâtiment 210, 91405 Orsay Cedex, France
[2] Department of Applied Mathematics and Theoretical Physics, University of Cambridge, Wilberforce Road, Cambridge CB3 0WA, UK
[3] Laboratoire de Physique Corpusculaire de Clermont-Ferrand, Unité Mixte de Recherche 6533 CNRS/IN2P3-Université Blaise Pascal, Campus des Cézeaux, 24 avenue des Landais, BP 80026, 63171 Aubière Cedex, France

Abstract We present two-flavor lattice QCD estimates of the hadronic couplings $g_{B_0^* B\pi}$ and $g_{B_1^* B_0^* \pi}$ that parametrize the non-leptonic decays $B_0^* \to B\pi$ and $B_1^* \to B_0^* \pi$. We use CLS two-flavor gauge ensembles. Our framework is the Heavy Quark Effective Theory (HQET) in the static limit and solving a Generalized Eigenvalue Problem (GEVP) reveals crucial to disentangle the $B_0^*(B_1^*)$ state from the $B\pi(B^*\pi)$ state. This work brings us some experience on how to treat the possible contribution from multihadronic states to correlation functions calculated on the lattice, especially when S-wave states are involved.

1 Introduction

Heavy Meson Chiral Perturbation Theory (HMχPT) [1,2] is commonly used to extrapolate lattice data in the heavy-light sector to the physical point. Relying on Heavy Quark Symmetry and the (spontaneously broken) chiral symmetry, an effective Lagrangian is derived where heavy-light mesons fields [3] couple to a Goldstone field via derivative operators. In the static limit, the total angular momentum of the light degrees of freedom, $\vec{j}_l = \vec{s}_l + \vec{L}$, is conserved independently of the total angular momentum $J = j_l \pm 1/2$. The pseudoscalar (B) and the vector (B^*) mesons belong to the doublet $j_l^P = (1/2)^-$ corresponding to $L = 0$ whereas the scalar (B_0^*) and the axial (B_1^*) mesons belong to the positive parity doublet $j_l^P = (1/2)^+$ corresponding to $L = 1$ (see Table 1). Equivalently to the low energy constants that parametrize the well-known chiral Lagrangian, hadronic couplings enter the effective theory under discussion, that is,

[a] e-mail: benoit.blossier@th.u-psud.fr
[b] On leave from School of Mathematics, Trinity College, Dublin 2, Ireland

particularly suitable to describe processes with emission of soft pions, i.e. $H_1(J_1) \to H_2(J_2)\pi$ where H_i is a heavy-light meson, and $p_\pi \ll \Lambda_\chi \sim 1$ GeV. The associated pionic couplings are $g_{H_1(J_1)H_2(J_2)\pi}$ and they cannot be computed in perturbation theory. When the negative $j^P = (1/2)^-$ and positive $j^P = (1/2)^+$ parity states are taken into account, the effective Lagrangian is parametrized by three couplings $\widehat{g}$, $\widetilde{g}$ and h. The first coupling, $\widehat{g}$, relates transitions between mesons belonging to the same doublet $J^P = (1/2)^-$ and has been precisely measured on the lattice [4–8]. On the contrary, the last two couplings are less precisely known. The residue at the poles of form factors in heavy to light semileptonic decays [9] is also expressed in terms of those couplings. In that respect, the channel $B_0^* \to B\pi$ is very interesting:

$$\Gamma(B_0^{*0} \to B^+\pi^-) = \frac{1}{8\pi} g_{B_0^* B\pi}^2 \frac{|\vec{q}_\pi|}{m_{B_0^*}^2},$$

$$|\vec{q}_\pi| = \frac{\sqrt{[m_{B_0^*}^2 - (m_B + m_\pi)^2][m_{B_0^*}^2 - (m_B - m_\pi)^2]}}{2 m_{B_0^*}}.$$

The HMχPT Lagrangian tells us that the transition reads also [10]

$$\Gamma(B_0^* \to B^+\pi^-) = \frac{h^2}{8\pi f_\pi^2} \frac{m_B}{m_{B_0^*}^3} \left(m_{B_0^*}^2 - m_B^2 \right)^2 |\vec{q}_\pi|,$$

by the identification

$$g_{B_0^* B\pi} = \sqrt{\frac{m_B}{m_{B_0^*}}} \left(m_{B_0^*}^2 - m_B^2 \right) \frac{h}{f_\pi},$$

which is appropriate in the heavy quark limit. In the static limit, the coupling $\widetilde{g}$ is similar to $\widehat{g}$, but for a hadronic transition between positive parity states. Those transitions are energetically not allowed for the B system but are useful for chiral extrapolations in Lattice QCD. So far there

Table 1 Quantum numbers of the ground state B meson and its first orbital excitations

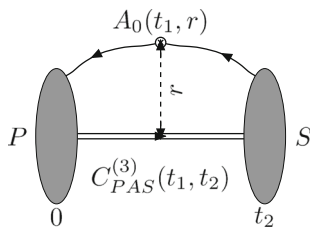| L	j_l^P	J^P	State
0	$(1/2)^-$	0^-	B
		1^-	B^*
1	$(1/2)^+$	0^+	B_0^*
		1^+	B_1^*

Fig. 1 Three-point correlation function used by [11] to compute $A_+(\Delta^2 = q^2)$

is only one computation of h and $\widetilde{g}$ [11], using ratio of three-point correlation functions and the techniques of measuring the Fourier transform of the radial distribution to obtain the form factor $A_+(q_\pi^2)$ in the limit $q_\pi^2 \to 0$, to extract h:

$$A_+(\delta^2 - q_\pi^2) = 4\pi \int_0^\infty r^2\, dr\, \frac{\sin(q_\pi r)}{q_\pi r} f_{PAS}(r),$$

where $\delta = m_{B_0^*} - m_B$, $f_{PAS}(r) = \langle B|[\bar{q}\gamma_0\gamma_5 q](r)|B_0^*\rangle$ is the radial distribution depicted in Fig. 1 and $\vec{q}_\pi = (0, 0, q_z)$, choosing $q_z = \delta$.

In Ref. [12] the transition $B_0^* \to B\pi$ was directly studied on the lattice, computing two-point correlation functions: the authors claimed that, close to the threshold $m_{B\pi} \sim m_{B_0^*}$, the ratio

$$C^{(2)}_{B_0^* B\pi}(t)/\sqrt{C^{(2)}_{B_0^* B_0^*}(t) C^{(2)}_{B\pi B\pi}(t)},$$

is related to $\Gamma(B_0^* \to B^+\pi^-)$. We follow here this last approach and perform the computation on a set of $N_f = 2$ configurations made available by the Lattice Coordinated Simulations effort. It gives a further check that the extraction of the scalar B meson decay constant on those ensembles, which we report in a forthcoming paper, is under control at ~10 % of precision we hope. The plan of the letter is the following: in Sects. 2 and 3 we describe the approach we have employed, in Sect. 4 we present our lattice set-up and our results are given in Sect. 5, which we discuss in Sect. 6.

2 Extraction of $\langle B\pi | B_0^* \rangle$

The transition amplitude under interest is parametrized by

$$\langle \pi^+(q_\pi) B^-(p)|B_0^{*0}(p')\rangle = g_{B_0^* B\pi}$$
$$= \sqrt{m_B m_{B_0^*}} \frac{m_{B_0^*}^2 - m_B^2}{m_{B_0^*}^2} \frac{h}{f_\pi},$$

with $q_\pi = p' - p$ and $f_\pi = 130$ MeV, the pion decay constant. When the transition amplitude is small, the Fermi golden rule teaches us that

$$\Gamma(B_0^* \to B^-\pi^+) = 2\pi \, |\langle \pi^+(q_\pi) B^-(p)|B_0^{*0}(p')\rangle|^2\, \rho,$$

where the density of states ρ reads, for a given energy E_π of the pion living on the lattice of spatial volume L^3,

$$\rho(E_\pi) = \frac{L^3}{(2\pi)^3} 4\pi \vec{q}_\pi^2 \frac{dq_\pi}{dE_\pi} = \frac{L^3}{2\pi^2} |\vec{q}_\pi| E_\pi.$$

In lattice units (a being the lattice spacing), we obtain

$$\frac{\Gamma(B_0^* \to B^-\pi^+)}{q_\pi} = \frac{1}{\pi}\left(\frac{L}{a}\right)^3$$
$$\times (aE_\pi)\, |a\langle \pi^+(q_\pi) B^-(p)|B_0^{*0}(p')\rangle|^2.$$

Considering the two-point correlation function $C^{(2)}_{B_0^* B\pi}(t) = \langle \mathcal{O}^{B\pi}(t)\mathcal{O}^{B_0^{*\dagger}}(0)\rangle$, where $O^{B_0^*}$ and $O^{B\pi}$ are interpolating fields with vanishing momentum of the B_0^* and the $B\pi$ states, respectively, we have

$$C^{(2)}_{B_0^* B\pi}(t) = \sum_{t_1} \langle 0|\mathcal{O}^{B_0^*}|B_0^*\rangle x \langle B\pi|\mathcal{O}^{B\pi}|0\rangle$$
$$\times e^{-m_{B_0^*} t_1} e^{-m_{B\pi}(t - t_1)} + \mathcal{O}(x^3) + \text{excited states},$$

with $x = |a\langle \pi^+(q_\pi) B^-(p)|B_0^{*0}(p')\rangle|$. We have assumed small overlaps $\langle 0|\mathcal{O}^{B_0^*}|B\pi\rangle$ and $\langle 0|\mathcal{O}^{B\pi}|B_0^*\rangle$ and the normalization of states is $\langle n|m\rangle = \delta_{mn}$. Finally, close to the threshold $m_{B_0^*} \approx m_{B\pi}$, we get

$$C^{(2)}_{B_0^* B\pi}(t) = \langle 0|\mathcal{O}^{B_0^*}|B_0^*\rangle x \langle B\pi|\mathcal{O}^{B\pi}|0\rangle \times t e^{-m_{B_0^*} t}$$
$$+ \mathcal{O}(x^3) + \text{excited states}.$$

Therefore, one can extract x from the ratio [13–15]

$$R(t) = \frac{C^{(2)}_{B_0^* B\pi}(t)}{\left(C^{(2)}_{B_0^* B_0^*}(t) C^{(2)}_{B\pi B\pi}(t)\right)^{1/2}} \approx A + xt, \qquad (1)$$

where $C^{(2)}_{B_0^* B_0^*}$ and $C^{(2)}_{B\pi B\pi}$ are, respectively, two-point correlation functions of a scalar B meson and a $B\pi$ multihadronic state:

$$C^{(2)}_{B_0^* B_0^*}(t) = \langle \mathcal{O}^{B_0^*}(t)\mathcal{O}^{B_0^{*\dagger}}(0)\rangle,$$
$$C^{(2)}_{B\pi B\pi}(t) = \langle \mathcal{O}^{B\pi}(t)\mathcal{O}^{B\pi\dagger}(0)\rangle.$$

Further away from the threshold, Eq. (1) has to be modified. The most interesting correction for our analysis is the one to the linear term in x. The time dependence of the ratio R is then in

$$t \longrightarrow \frac{2}{\Delta}\sinh\left(\frac{\Delta}{2}t\right) = t + \frac{\Delta^2 t^3}{24} + \mathcal{O}(\Delta^4), \qquad (2)$$

where $\Delta = m_{B_0^*} - m_{B\pi}$. To suppress the contamination by excited states, it is suitable to solve a Generalized Eigenvalue Problem (GEVP) [16–20]:

$$R^{\mathrm{GEVP}}(t) = \frac{\left(v_{B_0^*}(t,t_0),\, C^{(2)}_{B_0^* B\pi}(t) v_{B\pi}(t,t_0)\right)}{\sqrt{\left(v_{B_0^*}(t,t_0),\, C^{(2)}_{B_0^* B_0^*}(t) v_{B_0^*}(t,t_0)\right) \times \left(v_{B\pi}(t,t_0),\, C^{(2)}_{B\pi\, B\pi}(t) v_{B\pi}(t,t_0)\right)}}, \qquad (3)$$

where $C^{(2)}_{B_0^* B\pi}$, $C^{(2)}_{B_0^* B_0^*}$ and $C^{(2)}_{B\pi\, B\pi}$ are from now matrices of two-point correlators and v_X are the generalized eigenvectors associated to the ground state in the corresponding channel

$$C^{(2)}_{B_0^* B_0^*}(t) v_{B_0^*}(t,t_0) = \lambda_{B_0^*}(t,t_0) C^{(2)}_{B_0^* B_0^*}(t_0) v_{B_0^*}(t,t_0), \quad (4)$$

$$C^{(2)}_{B\pi\, B\pi}(t) v_{B\pi}(t,t_0) = \lambda_{B\pi}(t,t_0) C^{(2)}_{B\pi\, B\pi}(t_0) v_{B\pi}(t,t_0), \qquad (5)$$

and $(a, Cb) = \sum_i a_i C_{ij} b_j$ is the scalar product.

3 Extraction of $\widetilde{g}$

Similarly to the coupling $\widehat{g}$ which sets the magnitude of the transition between the pseudoscalar and the vector B mesons by exchanging a single soft pion [10], the coupling $\widetilde{g}$ parametrizes the amplitude

$$\langle B_0^* \,|\, \overline{\psi}_l \gamma_k \gamma_5 \psi_l \,|\, B_1^*(\epsilon_k)\rangle = \widetilde{g}\,\epsilon_k, \qquad (6)$$

where B_0^* and B_1^* are, respectively, the scalar and the axial B mesons at rest and ϵ_k is the polarization vector of the axial B meson. This matrix element can be extracted using the same technique as discussed in [19] but applied to the first excited heavy-light mesons doublet. Therefore following the method of [19,20], we consider the ratio of three- to two-point correlation functions

$$C^{(3)}_{ij}(t, t_1) = \frac{1}{V^3} \sum_{\vec{x},\vec{y},\vec{z}} \sum_{t_x} \langle \mathcal{O}_i^{B_0^*}(\vec{z}, t + t_x)$$
$$\times \mathcal{A}_k(\vec{y}, t_1 + t_x) \mathcal{O}_j^{B_1^{*\dagger}}(\vec{x}, t_x)\rangle, \qquad (9)$$

and $\mathcal{A}_k = Z_A \overline{\psi}_l(x) \Gamma_k^A \psi_l(x)$ is the renormalized axial current. The renormalization constant Z_A was determined non-perturbatively by the ALPHA Collaboration [21]. Here, $C^{(3)}(t, t_1)$ is again a matrix of correlators and the eigenvectors $v_{B_1^*}(t, t_0)$ are defined similarly to Eq. (4). Thanks to heavy quark symmetry, the two-point correlation functions $C^{(2)}_{B_0^* B_0^*}$ and $C^{(2)}_{B_1^* B_1^*}$ are proportional and only one GEVP needs to be solved. Finally, one can show that, in the static limit of HQET [19],

$$\mathcal{M}^{\mathrm{sGEVP}}(t, t_0) \xrightarrow[t_0=t-1]{t\gg1} \widetilde{g} + \mathcal{O}\left(t e^{-\Delta_{N+1,n} t}\right),$$

where $\Delta_{mn} = E_m - E_n$ is the energy difference between the mth and nth excited states of the GEVP and $N \times N$ is the size of the matrix of correlators defining the GEVP.

4 Lattice setup

In our study we have performed measurements on a subset of four $N_f = 2$ CLS lattice simulations, which have been generated using either the DD-HMC algorithm [22–25] or the MP-HMC algorithm [26], defined with the plaquette gauge action and non-perturbatively $\mathcal{O}(a)$ improved Wilson–Clover fermions; we collect the main parameters in Table 2 and we remind the reader that the criterion of our choice is to be very close to the threshold $m_{B_0^*} \approx m_{B\pi}$ (see Table 3). We have computed static-light correlators with HYP2 static quarks [27,28] and stochastic all-to-all propagators with full time dilution for the light quarks [29]. A single stochastic source has been used to compute the propagator. Interpolating fields of a static-light meson are defined as [30]

$$\mathcal{M}^{\mathrm{sGEVP}}(t, t_0) = -\partial_t \left(\frac{\left(v_{B_0^*}(t,t_0),\, \left[K(t)/\lambda_{B_0^*}(t,t_0) - K(t_0)\right] v_{B_1^*}(t,t_0)\right)}{\left(v_{B_0^*}(t,t_0),\, C^{(2)}_{B_0^* B_0^*}(t_0) v_{B_0^*}(t,t_0)\right)^{1/2} \left(v_{B_1^*}(t,t_0),\, C^{(2)}_{B_1^* B_1^*}(t_0) v_{B_1^*}(t,t_0)\right)^{1/2}} \right), \qquad (7)$$

where $K_{ij}(t)$ is the summed three-point correlation function

$$K_{ij}(t) = \sum_{t_1} C^{(3)}_{ij}(t, t_1), \qquad (8)$$

$$O^B_{\Gamma,n} = \overline{\psi}_l^{(n)} \Gamma \psi_h, \quad \psi_l^{(n)} \equiv (1 + \kappa_G a^2 \Delta)^{R_n} \psi_l, \qquad (10)$$

where ψ_h is the static heavy quark field and ψ_l is the relativistic quark field ($l = u/d$). The Gaussian smearing parameters

Table 2 Simulations parameters: the bare coupling constant $\beta = 6/g_0^2$, spatial extent in lattice units L (with $T = 2L$), hopping parameter κ, lattice spacing a in physical units, pion mass m_π and number of con-figurations used for the computation of the two-point and three-point correlation functions respectively

CLS label	β	$L^3 \times T$	κ	a [fm]	m_π [MeV]	$\#_h$	$\#_{\widetilde{g}}$
B6	5.2	$48^3 \times 96$	0.13597	0.075	280	250	200
E5	5.3	$32^3 \times 64$	0.13625	0.065	440	450	400
F6		$48^3 \times 96$	0.13635		310	300	250
N6	5.5	$48^3 \times 96$	0.13667	0.048	340	250	200

Table 3 Numerical values of ax, $\Gamma/|\vec{q}_\pi|$, $g_{B_0^* B\pi}$, $\delta = m_{B_0^*} - m_B$, $\Delta = m_{B_0^*} - m_{B\pi}$, h and $\widetilde{g}$ obtained on the four CLS ensembles that we have analyzed, with $m_{B_0^*} \approx m_B + m_\pi$

CLS	ax	$\Gamma/|\vec{q}_\pi|$	$g_{B_0^* B\pi}$ [GeV]	$a\delta$	$a\Delta$	h	$\widetilde{g}$
B6	−0.0156(4)	0.92(4)	27.4(0.1)(0.6)	0.141(4)	0.034(4)	0.85(3)(2)	−0.122(7)
E5	−0.0238(9)	0.86(7)	26.4(0.1)(1.0)	0.133(6)	−0.012(6)	0.82(3)(3)	−0.117(6)
F6	−0.0161(3)	0.95(3)	27.7(0.1)(0.5)	0.129(3)	0.025(3)	0.86(3)(2)	−0.119(4)
N6	−0.0172(6)	0.88(6)	26.6(0.1)(0.9)	0.092(3)	0.008(3)	0.82(3)(3)	−0.122(5)

are $\kappa_G = 0.1$, $r_n \equiv 2a\sqrt{\kappa_G R_n} \leq 0.6$ fm and Δ is a covariant Laplacian made of three times APE-blocked links [31]. Moreover, $O_{\Gamma,n}$ can be "local" ($\Gamma = \gamma_0, \gamma_5$) or contain a derivative operator ($\Gamma = \gamma_0 \sum_{i=1}^3 \gamma_i \nabla_i$, $\Gamma = \gamma_5 \sum_{i=1}^3 \gamma_i \nabla_i$) where ∇_i is the symmetrized covariant derivative acting on the light quark field: $\nabla_i \psi_l(x) = (U_i(x)\psi_l(x + \hat{i}) - U_i^\dagger(x)\psi_i(x - \hat{i}))/2$. We have also implemented the isosymmetric interpolating fields of the form

$$\mathcal{O}_n^{B\pi} = \frac{1}{V^2} \sum_{\vec{x}_1, \vec{x}_2} \sqrt{\frac{2}{3}} \left[\overline{\psi}_d(x_1)\gamma_5 \psi_u(x_1) \right] \left[\overline{\psi}_u^{(n)}(x_2)\gamma_5 \psi_h(x_2) \right]$$

$$- \sqrt{\frac{1}{6}} \left[\overline{\psi}_u(x_1)\gamma_5 \psi_u(x_1) - \overline{\psi}_d(x_1)\gamma_5 \psi_d(x_1) \right]$$

$$\times \left[\overline{\psi}_d^{(n)}(x_2)\gamma_5 \psi_h(x_2) \right],$$

which couple to the multihadronic state

$$\sqrt{\frac{2}{3}}\pi^+(0)B^-(0) - \sqrt{\frac{1}{3}}\pi^0(0)\overline{B}^0(0).$$

Using the notation $\overline{\psi_l^{(m)}(x)\psi_l^{(n)}}(y) = G_l^{mn}(x, y)$, $\overline{\psi_h(x)\psi_h}(y) = G_h(x, y)$ for the smeared light quark propagator and the static quark propagator, respectively, the two-point correlation functions constructed from these interpolating fields are

$$C_{B_0^* B_0^*}^{nm}(t) = -\frac{1}{V^2} \sum_{\vec{x}, \vec{y}} \text{Tr} \left[G_l^{mn}(y, x)\Gamma_1 G_h(x, y)\overline{\Gamma}_2 \right],$$

$$(11)$$

$\overline{\Gamma} = \gamma_0 \Gamma^\dagger \gamma_0$, whose the diagram is sketched in Fig. 2,
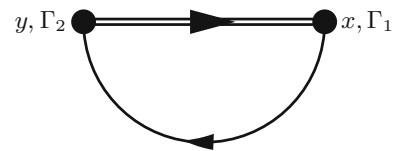

Fig. 2 Diagram representing the correlator $C_{B_0^* B_0^*}^{nm}$. The *simple* and *double lines* represent the light and static quark propagators respectively

$$C_{B\pi B\pi}^{nm}(t) = \frac{1}{V^4} \sum_{\vec{x}_i, \vec{y}_i} \text{Tr} \left[G_l(y_1, x_1)\gamma_5 G_l(x_1, y_1)\gamma_5 \right]$$

$$\times \text{Tr} \left[G_h(y_2, x_2)\gamma_5 G_l^{nm}(x_2, y_2)\gamma_5 \right] \quad (12)$$

$$- \frac{3}{2V^4} \sum_{\vec{x}_i, \vec{y}_i} \text{Tr} \left[G_l(y_1, x_1)\gamma_5 G_l^{0n}(x_1, x_2)\gamma_5 \right.$$

$$\left. \times G_h(x_2, y_2)\gamma_5 G_l^{m0}(y_2, y_1)\gamma_5 \right] \quad (13)$$

$$+ \frac{1}{2V^4} \sum_{\vec{x}_i, \vec{y}_i} \text{Tr} \left[G_l^{0n}(y_1, x_2)\gamma_5 G_h(x_2, y_2) \right.$$

$$\left. \times \gamma_5 G_l^{m0}(y_2, x_1)\gamma_5 G_l(x_1, y_1)\gamma_5 \right], \quad (14)$$

whose direct (12), box (13) and cross (14) diagrams are sketched in Fig. 3,

$$C_{B\pi B_0^*}^{nm}(t) = -\frac{1}{V^3}\sqrt{\frac{3}{2}} \sum_{\vec{x}_i, \vec{y}} \text{Tr}$$

$$\times \left[G_l^{m0}(y, x_1)\gamma_5 G_l^{0n}(x_1, x_2)\gamma_5 G_h(x_2, y)\overline{\Gamma} \right], \quad (15)$$

Fig. 3 Direct, *box* and *cross* diagrams contributing to the correlator $C^{nm}_{B\pi\,B\pi}$
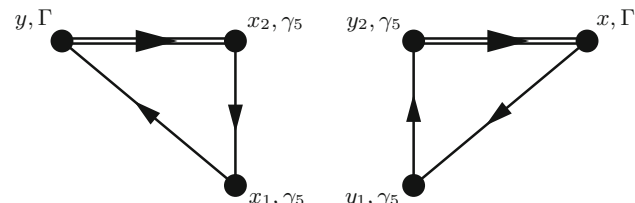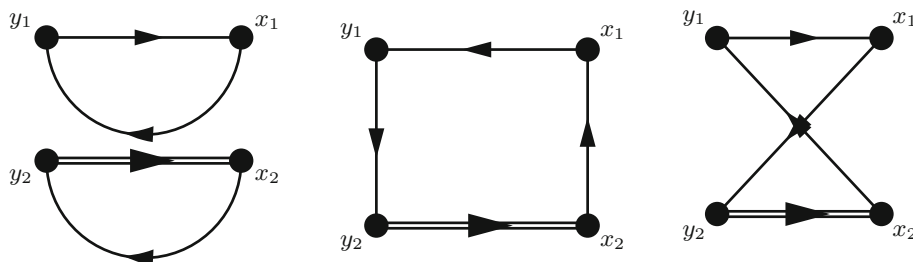
Fig. 4 Triangle diagrams contributing to the correlators $C^{nm}_{B\pi\,B^*_0}$ and $C^{nm}_{B^*_0\,B\pi}$

$$C^{nm}_{B^*_0\,B\pi}(t) = -\frac{1}{V^3}\sqrt{\frac{3}{2}}\sum_{\vec{y}_i,\vec{x}}\text{Tr}$$

$$\times\left[G^{m0}_l(y_2,y_1)\gamma_5 G^{0n}_l(y_1,x)\Gamma G_h(x,y_2)\gamma_5\right], \qquad (16)$$

whose the diagrams are sketched in Fig. 4. We have computed the triangle correlators $C_{B^*_0\,B\pi}$ and $C_{B\pi\,B^*_0}$ by two methods, either using the one-end-trick and a single inversion to obtain the two light propagators [32,33], or getting the second light propagator by solving the Dirac equation with the first light propagator taken as a generalized source. The second approach is more noisy, as shown on Fig. 5.
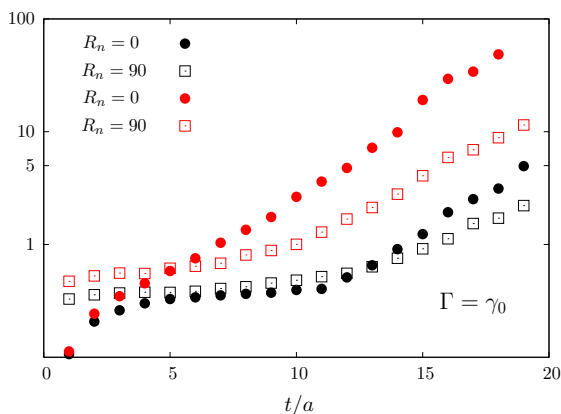
The box (13) and cross (14) diagrams depicted in Fig. 3 require at least one more inversion of the Dirac operator for each time slice and are therefore expensive to compute. They have been computed only in the case of the ensemble E5. Their contributions are small compared to the direct one given by (12), 0.1 and 1 %, respectively. Neglecting them, we obtain $ax = 0.0241(10)$ whereas we obtain $ax = 0.0228(10)$ when they are taken into account. The two results are compatible within our errors and the computation of these diagrams does not seem necessary at our level of precision. Since we do not expect the light quark mass dependence to play a major role on that specific point, we neglect these diagrams in our calculation on other ensembles.

Finally, we have also computed the three-point correlation functions (9) needed for the extraction of the coupling $\widetilde{g}$ using the same basis of interpolating operators:

$$C^{(3)}(t,t_1) = -\frac{Z_A}{V^3}\sum_{\vec{x},\vec{y},\vec{z}}\sum_{t_x}\frac{1}{3}$$

$$\times\sum_{k=1}^{3}\text{Tr}\left[G_h(x,z)\Gamma^A_k G^{n0}_l(z,y)\gamma_k\gamma_5 G^{0m}_l(y,x)\overline{\Gamma}^S\right],$$

where $\Gamma^S = \gamma_0,\ \gamma_i\overleftarrow{\nabla}_i$ and $\Gamma^A_i = \gamma_5\gamma_i,\ \gamma_5\overleftarrow{\nabla}_i$.
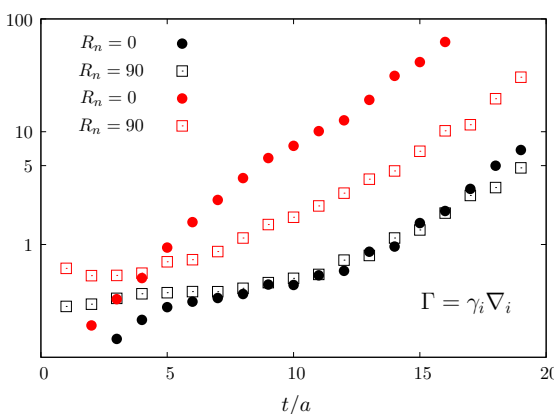

Fig. 5 Statistical error (in percent) for the correlation functions $C_{B^*_0\,B\pi}(t)$ for the two different methods explained in the text. The *black points* correspond to the correlators $C_{B^*_0\,B\pi}(t)$ computed using the one-end-trick and the *red points* correspond to the correlators $C_{B^*_0\,B\pi}(t)$ computed by inverting twice the Dirac operator. On the *left*, for $\Gamma = \gamma_0$ and on the *right*, for $\Gamma = \gamma_i\nabla_i$. The results correspond to the lattice ensemble E5

5 Results

We show in Fig. 6 the ratio $R^{\text{GEVP}}(t)$ and its derivative with respect to time $x^{\text{eff}}(t) = \mathrm{d}R^{\text{GEVP}}(t)/\mathrm{d}t$, which corresponds to the quantity ax we are measuring. We observe a nice plateau for every ensemble under study. The very flat behavior of $x^{\text{eff}}(t)$ in the plateau region lets us conclude that quadratic and higher terms in t in the formula Eq. (2), com-

ing from $\Delta \neq 0$ (see Table 3), are almost absent. This was expected, since in our range of fitting,

$$\frac{3t^2\Delta^2}{24} \ll 1 \quad \text{for } t/a \in [0 - 20].$$

Concerning the three-point correlation functions, we have checked using either local interpolating operators or interpolating operators built from the insertion of a covariant deriva-
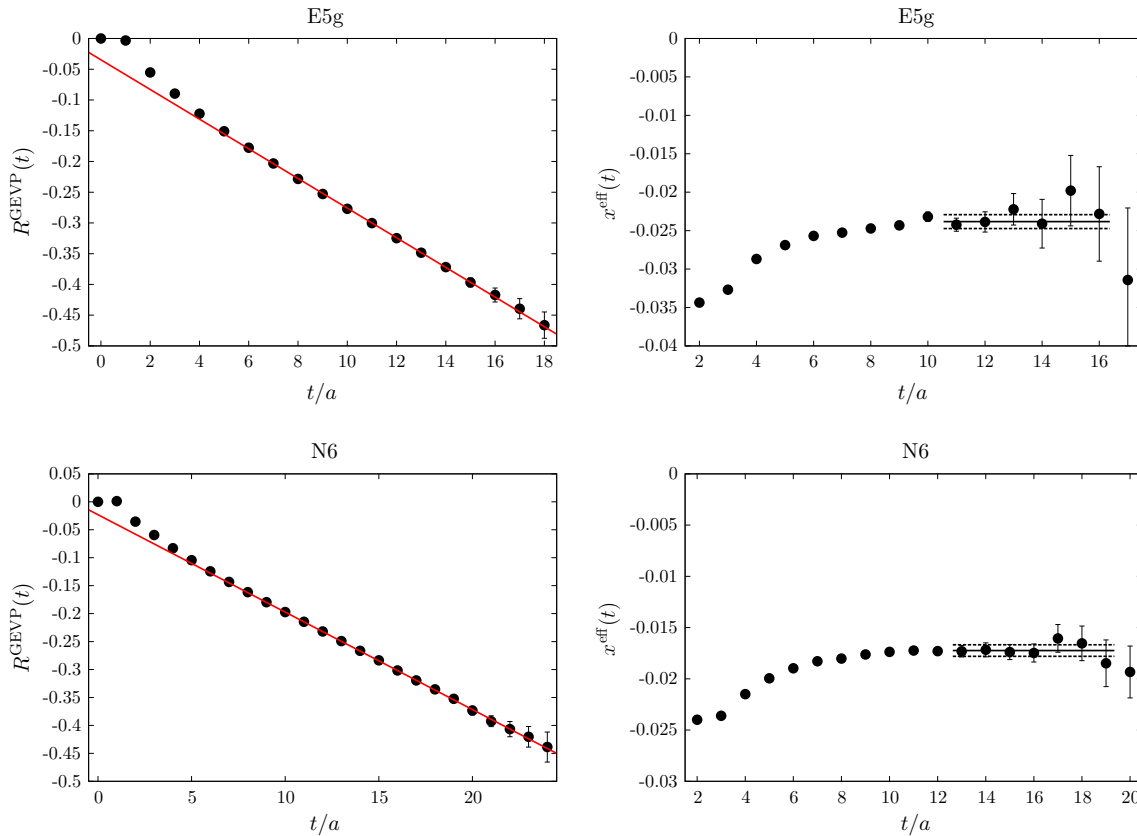

Fig. 6 On the *left*: evolution of $R^{\text{GEVP}}(t)$ with t/a for the CLS ensembles E5 and N6. The *red line* corresponds to a linear fit where the excited states contribution is negligible. On the *right*: the corresponding plateaus for $x^{\text{eff}}(t)$. We used $t_0/a = 5$ for $t > t_0$ and $t_0 = t - a$ elsewhere
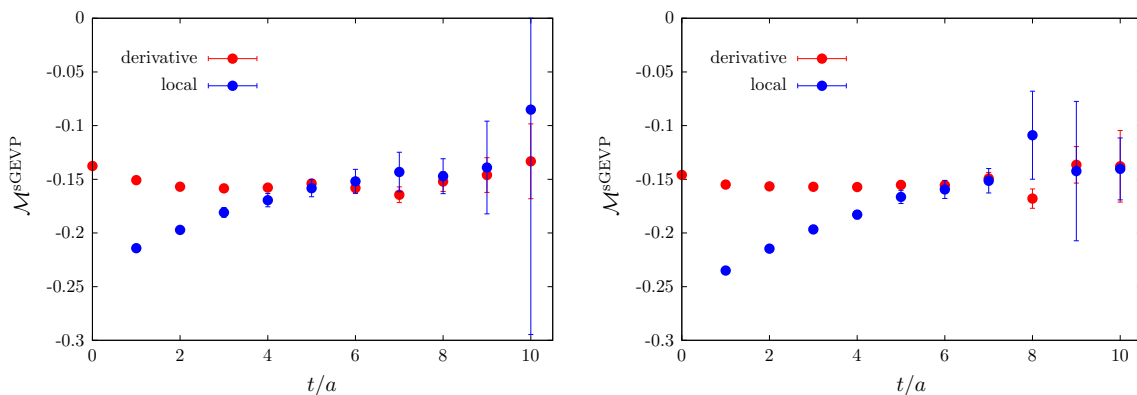

Fig. 7 Comparison of the signal obtained for $\mathcal{M}^{\text{sGEVP}}$ using local (*blue*) and derivative (*blue*) interpolating operators for the ensembles E5 (*left*) and F6 (*right*)
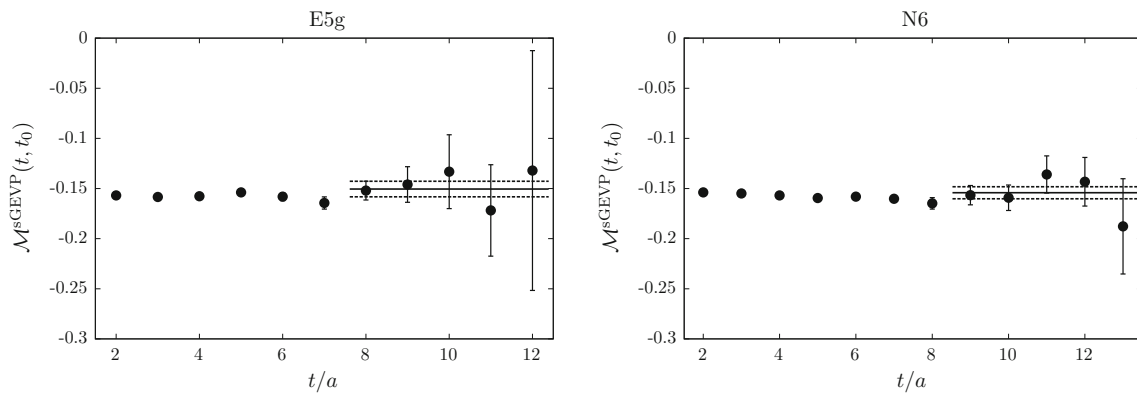
Fig. 8 Plateaus for $\mathcal{M}^{\mathrm{sGEVP}}$ using Eq. (7) for the CLS ensemble E5 (*left*) and N6 (*right*)
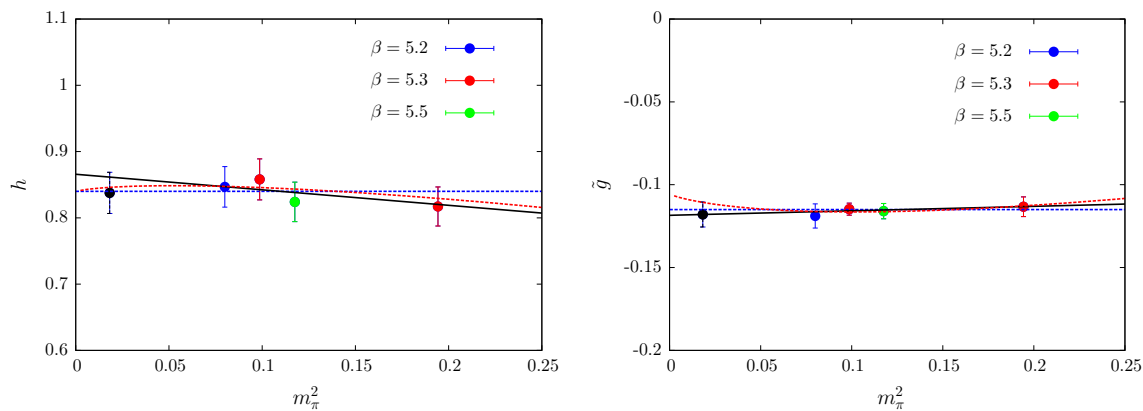

Fig. 9 Chiral extrapolations of the effective couplings h (*left*) and $\widetilde{g}$ (*right*). The *dashed blue line* corresponds to the constant fit, the *black line* corresponds to the linear fit and the *dashed red line* corresponds to the fit formulas (17), (18) with the expression derived in HMχPT

tive give compatible results. However, in the last case the signal is less noisy as shown in Fig. 7. Therefore only these fields are used in the following and some typical plateaus are depicted in Fig. 8.

With ax and $m_{B_0^*} - m_B = 385(17)_{\mathrm{stat}}(28)_{\mathrm{syst}}$ MeV [34], we can finally extract $\Gamma/|\vec{q}_\pi|$, h and $g_{B_0^* B\pi}$; we collect the values in Table 3. In the table, the first error on h comes from the uncertainty on $m_{B_0^*}$ in the continuum limit and the second error comes from the error on ax. The light-quark mass and lattice spacing dependence is so small on our data that it is legitimate to try a fit with a constant: we obtain $h = 0.84(3)$ and $\widetilde{g} = -0.120(3)$. Performing a linear fit in m_π^2, we get compatible results $h = 0.86(4)$ and $\widetilde{g} = -0.122(8)$. A third possibility is to use the NLO formulas of HMχPT [35]

$$
h = h_0 \left[1 - \frac{3}{4} \frac{3\widehat{g}_0^2 + 3\widetilde{g}_0^2 + 2\widehat{g}_0\widetilde{g}_0}{(4\pi f_\pi)^2} m_\pi^2 \log m_\pi^2 \right] + C_h m_\pi^2,
$$

$$(17)$$

$$
\widetilde{g} = \widetilde{g}_0 \left[1 - \frac{2 + 4\widetilde{g}_0^2}{(4\pi f_\pi)^2} m_\pi^2 \log(m_\pi^2) \right] + C_{\widetilde{g}} m_\pi^2, \quad (18)
$$

where $\widehat{g}_0 = 0.5(1)$ [4,8] is the pionic couplings associated to $H^* \to H\pi$. We get $h = 0.84(3)$ and $\widetilde{g} = -0.116(7)$. The previous formulas for $\widetilde{g}$ take into account corrections from tadpole diagrams to the axial coupling between $J = 0$ and $J = 1$ heavy-light mesons while Eq. (17) for h is obtained by considering directly the strong vertex $H_{J_1} \to H_{J_2}\pi$ [36]. The quark mass dependence is very small and the influence of the chiral logarithms does not change our result significantly. We quote finally

$$
h = 0.84(3)(2), \quad \widetilde{g} = -0.122(8)(6), \quad (19)
$$

where the first error is statistical and the second error corresponds to the uncertainty that we evaluate from the discrepancy between the constant and linear fits. We show in Fig. 9 the chiral extrapolations of h and $\widetilde{g}$. Rigorously, in the NLO chiral fits, we have neglected the contribution from the heavy-light states of opposite parity, as computed in [36]; they have been studied in [11]. Neglecting them is equivalent to assume $m_\pi \ll \delta = m_{B_0^*} - m_B$. Since, for our lattice ensembles, the pion mass lies in the range [280–440] MeV
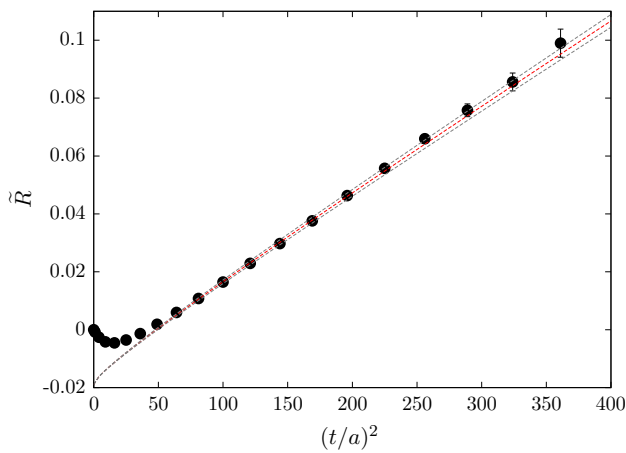
Fig. 10 Quadratic fit of $\widetilde{R}(t)$ for the CLS ensemble E5

and the mass difference between the scalar B meson and the ground state B meson is of the order of $\delta \sim 400$ MeV, the contribution is not negligible. Therefore, we also tried the other fit formulas:

$$
h = h_0 \left[1 - \frac{3}{4} \frac{3\widehat{g}_0^2 + 3\widetilde{g}_0^2 + 2\widehat{g}_0\widetilde{g}_0}{(4\pi f_\pi)^2} m_\pi^2 \log(m_\pi^2) \right.
$$
$$
\left. - \frac{h_0^2}{(4\pi f_\pi)^2} \frac{m_\pi^2}{2\delta^2} m_\pi^2 \log(m_\pi^2) \right] + C_h' m_\pi^2, \qquad (20)
$$

$$
\widetilde{g} = \widetilde{g}_0 \left[1 - \frac{2 + 4\widetilde{g}_0^2}{(4\pi f_\pi)^2} m_\pi^2 \log(m_\pi^2) \right.
$$
$$
\left. + \frac{h_0^2}{(4\pi f_\pi)^2} \frac{m_\pi^2}{8\delta^2} \left(3 + \frac{\widehat{g}_0}{\widetilde{g}_0} \right) m_\pi^2 \log(m_\pi^2) \right] + C_{\widetilde{g}}' m_\pi^2,
$$
$$
\qquad (21)
$$

where the coupling $\widehat{g}_0$ is the same as before and the mass difference δ is given in Table 3. The results are $h = 0.85(3)$ and $\widetilde{g} = -0.116(7)$ and is also perfectly compatible with our previous findings.

In Refs. [13,14], an alternative method to evaluate such a coupling like h was proposed. Indeed, one can show that the connected contribution to the correlation function $C_{B\pi\ B\pi}(t)$, which includes box (13) and cross (14) diagrams, has the following behavior:

$$
\widetilde{R}(t) = \frac{(v_{B\pi}(t), C_{\text{connected}}(t) v_{B\pi}(t))}{(v_{B\pi}(t), C_{B\pi\ B\pi}(t) v_{B\pi}(t))}
$$
$$
= A' + \frac{1}{2} x^2 t^2 + \mathcal{O}(t), \qquad (22)
$$

where $C_{\text{connected}}(t) = -\frac{3}{2} C_{\text{box}}(t) + \frac{1}{2} C_{\text{cross}}(t)$. As explained before, these diagrams have been computed only for the CLS ensemble E5 and the function $\widetilde{R}(t)$ is plotted in Fig. 10. The results are quite precise and the linear dependence in (22) cannot be neglected. Taking this into account, the result reads $|ax| = 0.0237(8)$, in perfect agreement with the one obtained

by the previous method (see Table 3). The fit range has been varied from $t/a \in [9-18]$ to $t/a \in [13-18]$ where the result is stable to estimate the error.

6 Discussion and conclusion

The couplings h and $\widetilde{g}$ were explicitly computed on the lattice in Ref. [11]. For h, two results are reported for the two different actions used there: $h = 0.69(2)(^{+11}_{-7})$ and $h = 0.58(2)(^{+6}_{-2})$. They are lower than what we get but this difference might be explained by the larger quark masses simulated at that time: indeed the chiral extrapolation tends to lower the extrapolated value. Our result is also a bit larger than the QCD sum rules estimates: in Ref. [37] the computation of $g_{B_0^* B\pi}$ gives $h = 0.56(28)$, while in Ref. [38] it gives $h = 0.74(23)$.

We can compare our finding with experimental data in the D sector, although the static approximation of HQET is expected to give only a rough estimate due to quite large $1/m_c$ corrections. For example, in the case of the D meson decay constant, a heavy quark spin breaking effects larger than 20 % between f_D and f_{D^*} has been measured [39]. With $m_{D_0^*} = 2318(29)$ MeV and $\Gamma_{D_0^*} = 267(40)$ MeV [40], we obtain $\Gamma(D_0^* \to D\pi)/|\vec{q}_\pi| = 0.68(11)$ and $h = 0.74(8)$, assuming that the branching ratio $\mathcal{B}(D_0^* \to D\pi)$ is ~ 100 %. This result is smaller than the one obtained in this work but it is compatible within error bars. In [41] the phase shift of the $D\pi$ scattering state was computed on the lattice: relating the coupling $g_{D_0^* D\pi}$ quoted in that paper to h, one finds that h is around 1.

Referring to the Adler–Weissberger sum rule [42–44] in the $B\pi$ system, in the $m_Q \to \infty$ and soft pion limits, $\sum_\delta |X_{B\delta}|^2 = 1$, where $\Gamma(\mathcal{I} \to \mathcal{F}\pi) = \frac{1}{2\pi f_\pi^2} \frac{|\vec{q}|^3}{2j_\mathcal{I}+1} |X_{\mathcal{I} \to \mathcal{F}}|^2$ [45], we have the bound $\widehat{g}^2 + h^2 < 1$. With the lattice average $\widehat{g} = 0.5(1)$ made with the results [4,8], we obtain the result that the sum rule would be saturated at 95 % by the B^* pole and the first orbital excitation.

We also confirm the finding of Ref. [11] where a small value of $\widetilde{g}$ was obtained. In particular this coupling for positive parity states is smaller than in the case of negative parity states $\widetilde{g} \ll g$.

In conclusion, we have extracted from lattice simulations with $N_f = 2$ dynamical quarks the couplings h and $\widetilde{g}$ that parametrize the emission of a soft pion by a scalar B meson. We have observed a very mild quark mass and cut-off dependence of our numbers and we quote $h = 0.84(3)(2)$, $\widetilde{g} = -0.122(8)(6)$ as our estimate. If $\widetilde{g}$ is small, the large value of h compared to $\widehat{g} \sim 0.5$ outlines the fact that some care is necessary to apply HMχPT for pion masses close to the mass splitting $m_{B_0^*} - m_B \sim 400$ MeV: B meson orbital excitation degrees of freedom cannot be neglected in chiral loops.

References

1. M.B. Wise, Phys. Rev. D **45**, 2188 (1992)
2. T.-M. Yan, H.-Y. Cheng, C.-Y. Cheung, G.-L. Lin, Y.C. Lin, H.-L. Yu, Phys. Rev. D **46**, 1148 (1992) [Erratum-ibid. D **55**, 5851 (1997)]
3. A.F. Falk, H. Georgi, B. Grinstein, M.B. Wise, Nucl. Phys. B **343**, 1 (1990)
4. H. Ohki, H. Matsufuru, T. Onogi, Phys. Rev. D **77**, 094509 (2008). arXiv:0802.1563 [hep-lat]
5. D. Becirevic, B. Blossier, E. Chang, B. Haas, Phys. Lett. B **679**, 231 (2009). arXiv:0905.3355 [hep-lat]
6. W. Detmold, C.D. Lin, S. Meinel, Phys. Rev. D **85**, 114508 (2012). arXiv:1203.3378 [hep-lat]
7. D. Becirevic, F. Sanfilippo, Phys. Lett. B **721**, 94 (2013). arXiv:1210.5410 [hep-lat]
8. F. Bernardoni, J. Bulava, M. Donnellan, R. Sommer (ALPHA Collaboration), Phys. Lett. B **740**, 278 (2015). arXiv:1404.6951 [hep-lat]
9. S. Descotes-Genon, A. Le Yaouanc, J. Phys. G **35**, 115005 (2008). arXiv:0804.0203 [hep-ph]
10. R. Casalbuoni, A. Deandrea, N. Di Bartolomeo, R. Gatto, F. Feruglio, G. Nardulli, Phys. Rep. **281**, 145 (1997). hep-ph/9605342
11. D. Becirevic, E. Chang, A. Le Yaouanc, arXiv:1203.0167 [hep-lat]
12. C. McNeile et al. (UKQCD Collaboration), Phys. Rev. D **70**, 054501 (2004). hep-lat/0404010
13. C. McNeile et al. (UKQCD Collaboration), Phys. Rev. D **63**, 114503 (2001). hep-lat/0010019
14. C. McNeile et al. (UKQCD Collaboration), Phys. Lett. B **556**, 177 (2003). hep-lat/0212020
15. C. McNeile et al. (UKQCD Collaboration), Phys. Rev. D **65**, 094505 (2002). hep-lat/0201006
16. C. Michael, Nucl. Phys. B **259**, 58 (1985)
17. M. Luscher, U. Wolff, Nucl. Phys. B **339**, 222 (1990)
18. B. Blossier, M. Della Morte, G. von Hippel, T. Mendes, R. Sommer, JHEP **0904**, 094 (2009). arXiv:0902.1265 [hep-lat]
19. J. Bulava, M. Donnellan, R. Sommer, JHEP **1201**, 140 (2012). arXiv:1108.3774 [hep-lat]
20. B. Blossier, J. Bulava, M. Donnellan, A. Gérardin, Phys. Rev. D **87**(9), 094518 (2013). arXiv:1304.3363 [hep-lat]
21. P. Fritzsch, F. Knechtli, B. Leder, M. Marinkovic, S. Schaefer, R. Sommer, F. Virotta, Nucl. Phys. B **865**, 397 (2012). arXiv:1205.5380 [hep-lat]
22. M. Lüscher, Comput. Phys. Commun. **156**, 209 (2004). hep-lat/0310048
23. M. Lüscher, Comput. Phys. Commun. **165**, 199 (2005). hep-lat/0409106
24. M. Lüscher, JHEP **0712**, 011 (2007). arXiv:0710.5417 [hep-lat]
25. M. Lüscher, DD-HMC algorithm for two-flavour lattice QCD. http://luscher.web.cern.ch/luscher/DD-HMC/index.html
26. M. Marinkovic, S. Schaefer, PoS LATTICE **2010**, 031 (2010). arXiv:1011.0911 [hep-lat]
27. A. Hasenfratz, F. Knechtli, Phys. Rev. D **64**, 034504 (2001). hep-lat/0103029
28. M. Della Morte, A. Shindler, R. Sommer, JHEP **0508**, 051 (2005). hep-lat/0506008
29. J. Foley, K. Jimmy Juge, A. O'Cais, M. Peardon, S.M. Ryan, J.-I. Skullerud, Comput. Phys. Commun. **172**, 145 (2005). hep-lat/0505023
30. S. Gusken, U. Low, K.H. Mutter, R. Sommer, A. Patel, K. Schilling, Phys. Lett. B **227**, 266 (1989)
31. M. Albanese et al. (APE Collaboration), Phys. Lett. B **192**, 163 (1987)
32. M. Foster et al. (UKQCD Collaboration), Phys. Rev. D **59**, 094509 (1999). hep-lat/9811010
33. C. McNeile et al. (UKQCD Collaboration), Phys. Rev. D **73**, 074506 (2006). hep-lat/0603007
34. D. Becirevic et al., in preparation
35. W. Detmold, C.-J.D. Lin, S. Meinel, Phys. Rev. D **84**, 094502 (2011). arXiv:1108.5594 [hep-lat]
36. S. Fajfer, J.F. Kamenik, Phys. Rev. D **74**, 074023 (2006). hep-ph/0606278
37. P. Colangelo, F. De Fazio, G. Nardulli, N. Di Bartolomeo, R. Gatto, Phys. Rev. D **52**, 6422 (1995). hep-ph/9506207
38. T.M. Aliev, M. Savci, J. Phys. G **22**, 1759 (1996). hep-ph/9604258
39. D. Becirevic, V. Lubicz, F. Sanfilippo, S. Simula, C. Tarantino, JHEP **1202**, 042 (2012). arXiv:1201.4039 [hep-lat]
40. J. Beringer et al. (Particle Data Group Collaboration), Phys. Rev. D **86**, 010001 (2012)
41. D. Mohler, S. Prelovsek, R.M. Woloshyn, Phys. Rev. D **87**(3), 034501 (2013). arXiv:1208.4059 [hep-lat]
42. S.L. Adler, Phys. Rev. **140**, B736 (1965) [Erratum-ibid. **149**, 1294 (1966); Erratum-ibid. **175**, 2224 (1968)]
43. S.L. Adler, Phys. Rev. **169**, 1392 (1968)
44. W.I. Weisberger, Phys. Rev. Lett. **14**, 1047 (1965)
45. D. Becirevic, A. Le Yaouanc, JHEP **9903**, 021 (1999). hep-ph/9901431